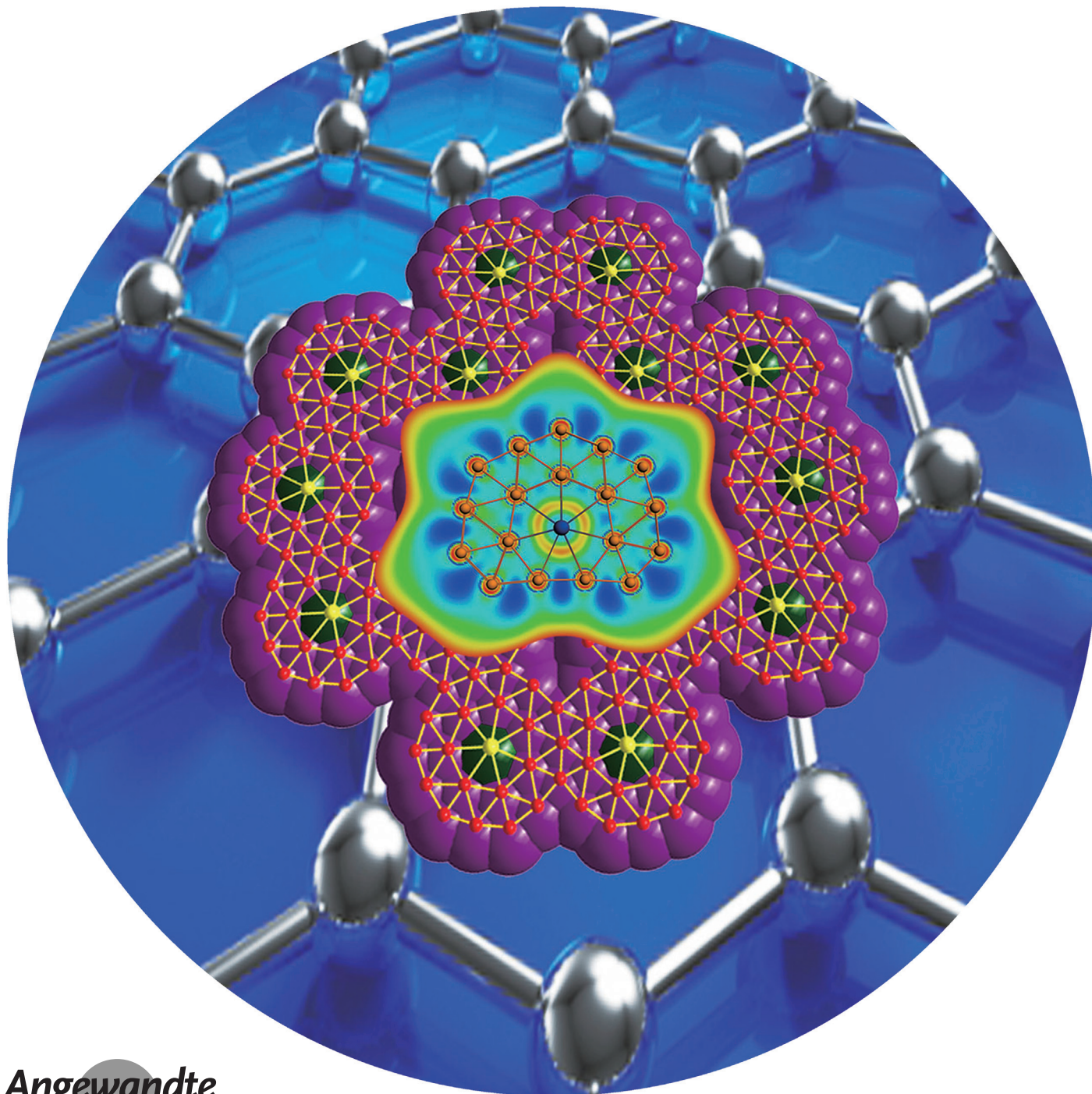


Metallo-Borophene

International Edition: DOI: 10.1002/anie.201601548
German Edition: DOI: 10.1002/ange.201601548

The Planar CoB_{18}^- Cluster as a Motif for Metallo-Borophenes

Wan-Lu Li⁺, Tian Jian⁺, Xin Chen, Teng-Teng Chen, Gary V. Lopez, Jun Li,^{*} and Lai-Sheng Wang^{*}



Abstract: Monolayer-boron (borophene) has been predicted with various atomic arrangements consisting of a triangular boron lattice with hexagonal vacancies. Its viability was confirmed by the observation of a planar hexagonal B_{36} cluster with a central six-membered ring. Here we report a planar boron cluster doped with a transition-metal atom in the boron network (CoB_{18}^-), suggesting the prospect of forming stable hetero-borophenes. The CoB_{18}^- cluster was characterized by photoelectron spectroscopy and quantum chemistry calculations, showing that its most stable structure is planar with the Co atom as an integral part of a triangular boron lattice. Chemical bonding analyses show that the planar CoB_{18}^- is aromatic with ten π -electrons and the Co atom has strong covalent interactions with the surrounding boron atoms. The current result suggests that transition metals can be doped into the planes of borophenes to create metallo-borophenes, opening vast opportunities to design hetero-borophenes with tunable chemical, magnetic, and optical properties.

The electron deficiency of boron gives rise not only to a variety of polymorphs in the bulk,^[1] but also diverse chemistries with unusual structures and multi-center bonding.^[2] In the molecular and nano-scale, boron also displays interesting chemical structures and bonding. Over the past decade, joint experimental and theoretical studies have uncovered a fascinating landscape for size-selected boron clusters, ranging from planar structures to fullerene-like cage structures (borospherenes).^[3–6] In contrast to bulk boron, size-selected boron clusters (B_n^-) have been found to be planar or quasi-planar (2D) up to 27 atoms as anions,^[7] and continue to be 2D at $n = 30, 35,$ and $36.$ ^[8–10] Due to its electron deficiency, boron cannot form hexagonal monolayers like graphene, whereas a triangular boron lattice obtained by filling a hexagonal boron layer was predicted to be buckled.^[11–14] Perfectly planar monolayers were predicted for a triangular boron lattice with hexagonal holes.^[15,16] Monolayer boron structures with various hole patterns and densities, as well as their possible realization on suitable substrates, in particular Ag-(111), have been considered computationally.^[17–21] The remarkable finding of the planar B_{36} and B_{36}^- clusters with a central hexagonal hole provided the first experimental evidence for the viability of perfectly planar boron monolayers, which we firstly named borophenes.^[10,22] Recently, borophenes have been synthesized by atomic deposition on a silver surface by Mannix et al.^[23] Comparison of high-

resolution STM images with theoretical simulations concluded that the monolayer boron consisted of a buckled triangular lattice.^[23] A very recent independent study by Feng et al. using similar methods has reported borophenes on silver surfaces with hexagonal holes.^[24] Another recent study by Tai et al. reported the formation of γ - B_{28} 2D films on a copper surface consisting of B_{12} cages intercalated by B_2 units.^[25] These rapid progresses in experimental syntheses have paved the way for possible applications of borophenes in nanoscience and nanotechnologies.

Unlike graphene, borophenes seem to exhibit remarkable structural diversities. A key question is whether hetero-atoms can be doped into the planes of borophenes, as a new means of tuning the properties of borophenes unavailable for graphene. Following the finding of the planar wheel structures of the B_8^- and B_9^- clusters,^[26] which consisted of a monocyclic boron ring with a central boron atom ($B@B_n^-$), similar metal-doped boron rings were considered computationally.^[27–29] While main group elements, such as Al, were found to be unfavorable in the central position,^[30–32] a series of transition metal doped boron molecular wheels ($M@B_n^-$, $n = 8–10$) were produced and characterized both experimentally and theoretically.^[33] The $Nb@B_{10}^-$ and $Ta@B_{10}^-$ clusters were the largest borometallic wheels, setting a record of coordination number in 2D chemical systems.^[34] Larger doped boron clusters, such as CoB_{12}^- and RhB_{12}^- , were found to have half-sandwich-like structures with the metal atoms coordinated above the quasi-planar bowl-shaped B_{12} unit.^[35,36] Larger metal-doped boron clusters have been considered computationally, including the Fe-centered B_{14} and B_{16} double rings, and metal-centered B_{18} , B_{20} , and B_{24} cages.^[37,38]

Even though the proposed fullerene-like B_{80} was shown to be a high energy isomer,^[39] the recent discovery of borospherenes^[6,40] suggested the possibility of endohedral borospherenes,^[41–43] like the family of endohedral fullerenes.^[44] The viability of endohedral borospherenes requires the systematic characterization of doped boron clusters. Recently, the observation and characterization of the largest doped-boron clusters, CoB_{16}^- , was reported, revealing a remarkable drum-like structure with the Co atom coordinated by two connected B_8 rings.^[45] Here we report the next largest doped-boron cluster, CoB_{18}^- , which has been characterized by photoelectron spectroscopy and theoretical calculations. Surprisingly, rather than forming the anticipated drum-like structure, the CoB_{18}^- cluster is found to be a perfectly planar cluster with the Co atom as an integrated part of a triangular network of boron atoms ($Co@B_{18}^-$). The hetero-atom allows enough bond length flexibility, such that a perfectly planar structure is achieved without any defects (i.e. all B_3 triangles) in the boron lattice. The Co atom is found to engage in strong covalent interactions with the seven boron atoms in its first coordination shell. Chemical bonding analyses reveal that the planar CoB_{18}^- cluster is aromatic with ten π -electrons. The observation of a transition metal atom doped in the network of a planar boron cluster is unprecedented, suggesting the possibility of a new class of hetero-borophenes and metallo-borophenes.

The CoB_{18}^- cluster was produced by laser vaporization of a boron/cobalt composite target and characterized by photo-

[*] W. L. Li,^[†] X. Chen, Prof. Dr. J. Li

Department of Chemistry and Key Laboratory of Organic Optoelectronics & Molecular Engineering of Ministry of Education
Tsinghua University
Beijing 100084 (China)
E-mail: junli@tsinghua.edu.cn

T. Jian,^[†] T. T. Chen, Dr. G. V. Lopez, Prof. Dr. L. S. Wang
Department of Chemistry, Brown University
Providence, RI 02912 (USA)
E-mail: Lai-Sheng_Wang@brown.edu

[†] These authors contributed equally to this work.

Supporting information and the ORCID identification number(s) for the author(s) of this article can be found under <http://dx.doi.org/10.1002/anie.201601548>.

electron spectroscopy (PES), as shown in Figure 1a. The 193 nm spectrum revealed extremely high electron binding energies for CoB_{18}^- with six relatively well-resolved bands labeled as X and A–E. The X band designates the detachment

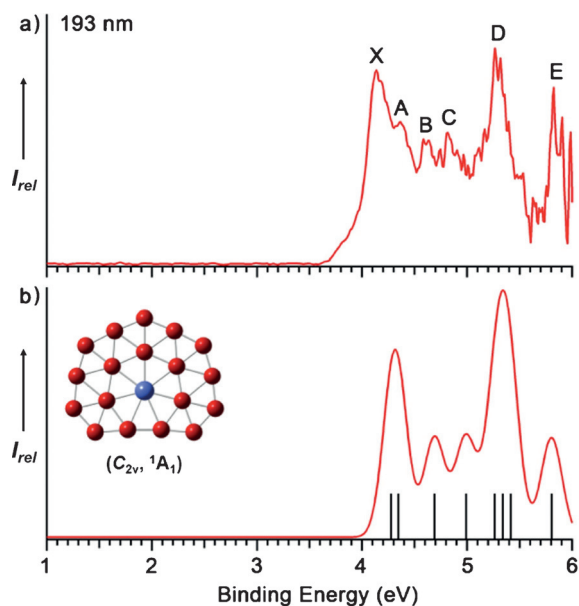


Figure 1. a) Photoelectron spectrum of CoB_{18}^- at 193 nm; b) The simulated spectrum from the global minimum planar structure of CoB_{18}^- by fitting the calculated VDEs (vertical bars) with a unit area Gaussian function of 0.15 eV width.

transition from the ground state of the anion to that of the neutral, while bands A–E denote detachment transitions to excited states of the neutral. Since no vibrational structures were resolved, the first adiabatic detachment energy (ADE) was estimated from the leading edge of the X band as 4.0 eV, which also represents the electron affinity (EA) of the neutral CoB_{18} cluster. The vertical detachment energy (VDE) was measured from the maximum of each band. The VDE of the X band was measured as 4.14 eV. The VDEs of all resolved PES bands are summarized in Table 1, where they are compared with the theoretical data. The intense band D at 5.3 eV was quite broad, suggesting it might contain multiple detachment transitions. Above 5.5 eV, the PES signal-to-noise ratios were poor, as seen by the spikes around band E. The first ADE of CoB_{18}^- at 4.0 eV is extremely high, in comparison to that of CoB_{16}^- at 2.48 eV,^[45] suggesting that CoB_{18}^- is a very stable electronic system.

We searched for the global minimum of CoB_{18}^- using a guided basin-hopping program called TGmin,^[10] as well as manual structural constructions (see the Supporting Information for details). More than 5000 structures with different spin states were generated from TGmin and further optimized at the levels of PBE, PBE0, and CCSD(T). The T_1 diagnostic values were found to be negligible in the CCSD(T) calculations, implying that the relative energies of the isomers were credible from the single-determinant methods. Vibrational frequencies were computed to verify the minima on the potential surface. The structures and energies of the global

Table 1: Theoretical VDEs [eV] of CoB_{18}^- and final electronic configurations at TDDFT-SAOP/TZP level compared with experimental results.

Observed band	VDE (exp) ^[a]	State	Final electron configurations	VDE (theo)
X ^[b]	4.14(6)	2A_1	...10b ₂ ² 11b ₂ ² 2a ₂ ² 3b ₁ ² 3a ₂ ² 13a ₁ ² 4b ₁ ² 14a₁¹	4.28
A	4.36(6)	2B_1	...10b ₂ ² 11b ₂ ² 2a ₂ ² 3b ₁ ² 3a ₂ ² 13a ₁ ² 4b₁¹14a₁²	4.35
B	4.62(5)	2A_1	...10b ₂ ² 11b ₂ ² 2a ₂ ² 3b ₁ ² 3a ₂ ² 13a₁¹4b₁²14a₁²	4.69
C	4.82(5)	2A_2	...10b ₂ ² 11b ₂ ² 2a ₂ ² 3b ₁ ² 3a₂¹13a₁²4b₁²14a₁²	4.99
D	5.30(5)	2B_1	...10b ₂ ² 11b ₂ ² 2a ₂ ² 3b₁¹3a₂²13a₁²4b₁²14a₁²	5.26
		2A_2	...10b ₂ ² 11b ₂ ² 2a₂¹3b₁²3a₂²13a₁²4b₁²14a₁²	5.34
		2B_2	...10b ₂ ² 11b₂¹2a₂²3b₁²3a₂²13a₁²4b₁²14a₁²	5.42
E	5.8(1)	2B_2	... 10b₂¹11b₂²2a₂²3b₁²3a₂²13a₁²4b₁²14a₁²	5.80

[a] Numbers in the parentheses are the uncertainty in the last digit. [b] The first experimental ADE of CoB_{18}^- or the EA of CoB_{18} is 4.00 ± 0.06 eV.

[b] The orbitals shown in bold face indicate the major electron detachment channels.

minimum of CoB_{18}^- and selected isomers are shown in Figure 2. All low-lying isomers within 50 kcal mol⁻¹ of the global minimum at the PBE level are given in Figure S1 of the Supporting Information. The global minimum of CoB_{18}^- is

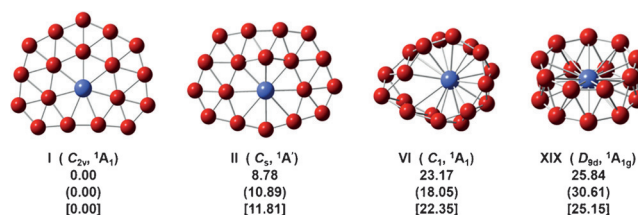


Figure 2. The global minimum of CoB_{18}^- and selected low-lying isomers. The energies obtained from CCSD(T), PBE/TZP (in parentheses), and PBE0/TZP (in brackets) are given in kcal mol⁻¹.

found unexpectedly to be a perfectly planar and closed-shell species with C_{2v} (1A_1) symmetry. In fact, the first five low-lying structures are all found to be planar (Figure S1). The nearest competing isomer II lies almost 9 kcal mol⁻¹ higher in energy than the global minimum at the CCSD(T) level, confirming the high stability of the planar C_{2v} structure of CoB_{18}^- . Importantly, the D_{9d} drum structure of CoB_{18}^- (isomer XIX) is found to be quite unfavorable, being higher in energy than the global minimum by 25.84 kcal mol⁻¹ at the CCSD(T) level (Figure 2).

To verify the planar global minimum of CoB_{18}^- , we calculated its VDEs using the scalar relativistic Δ SCF-TDDFT method^[46,47] with the SAOP density functional,^[48] as compared with the experimental data in Table 1 and Figure 1b. The first ADE is calculated as the total energy difference of CoB_{18}^- and CoB_{18} at their respective optimized geometries. The first VDE and the ADE calculated using the PBE/TZP, PBE0/TZP and CCSD(T) methods are compared with the experimental data in Table S1; the CCSD(T) results are in good agreement with the experiment. The structure of neutral CoB_{18} ($C_s, ^2A'$) is similar to the anion with very slight out-of-plane distortions (Figure S2), resulting in the relatively

sharp X band in the PES spectrum. Under the one-electron approximation, the first PES band corresponds to electron detachment from the $14a_1$ orbital (HOMO) composed mainly of Co $3d_{z^2}$ (Figures S3 and S4). The next three detachment channels, corresponding to bands A, B, C in the PES spectrum, are derived from electron detachments from the $4b_1$, $13a_1$, and $3a_2$ orbitals with calculated VDEs of 4.35, 4.69, and 4.99 eV, respectively, which agree well with the experimental results (Table 1). The three detachment channels from the $3b_1$, $2a_2$, and $11b_2$ orbitals yield similar VDEs, in excellent agreement with the intense and broad band D in the PES spectrum. The next calculated detachment transition is at 5.80 eV from the $10b_2$ orbital, in excellent agreement with band E at 5.8 eV. The VDEs are fitted with unit area Gaussian functions of 0.15 eV width to produce a simulated PES spectrum, as shown in Figure 1b. The overall agreement between experiment and theory as shown in both Figure 1b and Table 1 is excellent, confirming unequivocally the C_{2v} planar global minimum of CoB_{18}^- .

We also computed the VDEs from the isomers II, VI, and the drum-like isomer XIX (Figure 1), as given in Table S2. The simulated PES spectra using these VDEs for isomers II, VI and XIX are compared with the experimental spectrum in Figure S5. Clearly, these results totally disagree with the experiment and they can all be ruled out. VDEs of all these isomers are much lower in comparison with the experiment; in particular, the drum-like 3D structures VI and XIX have very low VDEs.

The detailed structural parameters of the anion and neutral species are given in Figure S2. The structures of the anion and neutral are very similar, except a very small out-of-plane distortion in the neutral. The peripheral B–B bond lengths in CoB_{18}^- are between 1.56 Å and 1.65 Å, smaller than those of the interior B–B bonds (1.66–1.90 Å), consistent with those found for bare planar boron clusters.^[3–10] The seven Co–B bond lengths range from 1.91 Å to 2.08 Å, which are close to the Co–B single bond length (1.96 Å) using the self-consistent covalent radii of Pyykkö.^[49] Therefore, the Co atom has optimal bonding with the seven boron atoms in its first coordination shell, giving rise to the high stability of the planar CoB_{18}^- cluster. It should be pointed out that $Co@B_8^-$ was found previously to be a highly stable borometallic molecular wheel with D_{8h} symmetry, in which the B–B and Co–B bond lengths are 1.56 and 2.03 Å, respectively.^[50] On the other hand, no $Co@B_7^-$ molecular wheel could exist because a bare B_7 ring would be too small to host the Co atom.^[51] However, in CoB_{18}^- , six of the seven B–B bonds in the first coordination shell of Co are interior bonds within the cluster plane with longer B–B bond lengths (>1.7 Å), which create a perfect space to fit the Co atom to allow optimal covalent interactions with the surrounding boron atoms. In contrast, the isomer II with Co coordinated by eight B atoms lies higher in energy (Figure 2).

Using the spin-restricted open-shell ROCCSD(T) method, we calculated the binding energy of $Co(3d^74s^2) + B_{18}^- (^2A_1) \rightarrow CoB_{18}^- (^1A_1)$ to be $162.46 \text{ kcal mol}^{-1}$ with zero-point-energy correction, which quantitatively measures the bonding strength between the central Co and the B_{18}^- host. The optimized structure of the bare planar $C_{2v} B_{18}^-$ cluster

with the framework of the CoB_{18}^- complex by removing the Co atom lies higher in energy by $49.41 \text{ kcal mol}^{-1}$ than the C_{3v} global minimum^[52] at the level of PBE0/TZP. The $C_{2v} B_{18}^-$ cluster is stabilized significantly by the doping of a Co atom with additional electrostatic stabilization via an electron transfer from Co to the B_{18} moiety, resulting effectively in a $Co^+@B_{18}^{2-}$ cluster (see below). Thus, both the covalent and electrostatic interactions between Co and the B_{18} host make CoB_{18}^- a highly thermodynamically stable species.

The optimal B–B and Co–B bond length constraints can also be used to understand why the D_{9d} drum isomer of CoB_{18}^- lies much higher in energy. In the recently reported CoB_{16}^- drum,^[45] the B–B bond length in each B_8 ring was 1.59 Å and the inter-ring B–B bond length was 1.80 Å, giving rise to a Co–B bond length of 2.22 Å. Even though this Co–B bond length was larger than the Co–B single bond length, the high coordination number was sufficient to yield a large binding energy between Co and the B_{16} drum host. However, in the $D_{9d} CoB_{18}^-$ drum isomer (XIX in Figure 2), the Co–B bond length becomes 2.45 Å, which is too large for Co to overlap effectively with the B atoms, making the drum isomer much higher in energy compared with the C_{2v} planar global minimum. It is also notable that the lowest 3D isomer VI (Figure 2) involves a CoB_{16}^- drum with two B atoms outside and it is more stable than the D_{9d} drum isomer. Hence, the Co–B interactions are critical in determining the structures of Co doped boron clusters.

To further understand the structure and stability of CoB_{18}^- , we analyzed its chemical bonding using the adaptive natural density partitioning (AdNDP) method at the level of PBE0/Def2-TZVP.^[53] The AdNDP analyses yield both localized and delocalized multi-center bonds, providing a chemically intuitive bonding picture for complicated molecular systems. The AdNDP analyses transform the 32 canonical molecular orbitals of CoB_{18}^- (Figure S4) into three types of bonds, as shown in the three rows of Figure 3. The first row depicts three 3d lone pairs on Co ($3d_{z^2}$, $3d_{xz}$ and $3d_{yz}$) with the occupation numbers (ONs) ranging from $1.83\text{--}1.99|e|$, compared to $2.00|e|$ in the ideal case, which means that $0.01\text{--}0.17|e|$ participates in π bonding with the surrounding boron atoms. The other two 3d orbitals ($3d_{x^2-y^2}$ and $3d_{xy}$) of Co participate in σ bonding with the seven surrounding B atoms, as displayed in the middle row of Figure 3.

The middle row displays three types of σ bonds, including thirteen $2c\text{--}2e$ B–B σ bonds involving the 13 peripheral B atoms with high ON of $1.82\text{--}1.92|e|$. These peripheral bonds are very similar to the peripheral bonds of bare planar boron clusters, except the B–B bond that is directly coordinated to Co but without a second coordination shell. This B–B bond has a longer bond length (1.65 Å, see Figure S2) and involves partially three-center bonding with the Co atom. The Co atom is bonded with the surrounding B_7 ring primarily via six $4c\text{--}2e$ bonds involving the $3d_{x^2-y^2}$ and $3d_{xy}$ orbitals. The inner B_7 ring and the outer eleven B atoms are bonded via five $4c\text{--}2e$ delocalized σ bonds. The third row in Figure 3 shows five globally delocalized π bonds, which fulfill the $(4n+2)$ Hückel rule for aromaticity. The optimal Co– B_7 covalent bonding in the C_{2v} global minimum of CoB_{18}^- and the aromatic characters are the major factors for its high stability.

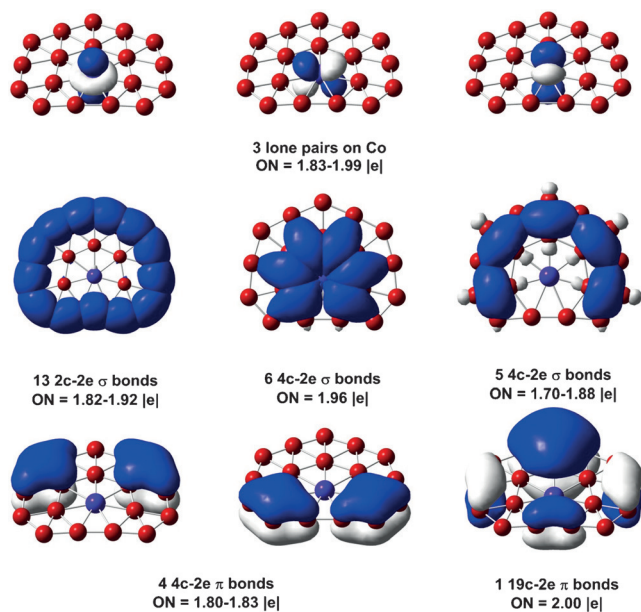


Figure 3. Chemical bonding analyses of CoB_{18}^- using AdNDP at the PBE0/Def2-TZVP level.

In the C_{2v} global minimum of CoB_{18}^- , the five 3d orbitals from Co transform as $a_1(d_{z^2})$, $b_1(d_{xz})$, $a_2(d_{yz})$, $a_1(d_{x^2-y^2})$, and $b_2(d_{xy})$, with the z -axis perpendicular to the B_{18} framework (Figure S3). From the Kohn–Sham MO analyses, the $3d_{z^2}$, $3d_{xz}$ and $3d_{yz}$ orbitals remain nearly doubly occupied, whereas the $3d_{xy}$ and $3d_{x^2-y^2}$ orbitals directly interact with the B 2p orbitals in the molecular plane (Figure S3), as also revealed in the AdNDP analyses (Figure 3). By integrating the populations of electrons, we find that there are two electrons derived from the $3d_{xy}$ and $3d_{x^2-y^2}$ orbitals of Co in the occupied region. Mulliken population analyses also show that the valence electron density on the Co 3d orbitals is 8.09. Therefore, CoB_{18}^- is a d^8 -complex with Co in a rare oxidation state of +1 and can be viewed approximately as $\text{Co}^+\text{B}_{18}^{2-}$ with additional ionic bonding. This species thus adds to the family of unusual monovalent transition metal cluster compounds.^[54,55] As the CoB_{18}^- anion is closed shell, the neutral CoB_{18} is thus open-shell with an unpaired 3d electron and should be magnetic.

The doping of a transition-metal atom into the plane of a boron network is unprecedented and is a significant experimental observation. In size-selected boron clusters for $n > 9$, truly planar structures always involve a tetragonal, pentagonal, or hexagonal defects.^[5–10] A triangular lattice always display out-of-plane distortions, just like in the infinitely large monolayer boron with a triangular lattice.^[11–14] In the finite system, the peripheral B–B bonds are stronger with shorter bond lengths due to dangling bonds, which create strains in the interior of the planar boron clusters. This strain can be released either by out-of-plane distortions or non-triangular defects. However, in the C_{2v} planar CoB_{18}^- the Co–B bond distance is longer than typical interior B–B bonds, and, therefore, the hetero-atom helps relieve the strain created by the short peripheral B–B bonds to allow a perfectly planar structure. This observation suggests that different

transition-metal or f-element atoms may be doped into monolayer borons to create hetero-borophenes. Thus, doping can be another handle to tune the properties of borophenes, which is not available to graphene. With transition metals and rare-earth elements, it is conceivable to create metallo-borophenes with tunable magnetic, optical, and non-linear optical properties. The low oxidation state observed for the Co atom in CoB_{18}^- suggests that such metallo-borophenes may also have interesting chemical and catalytic properties.

In summary, we have observed a unique planar CoB_{18}^- cluster, in which the Co atom is directly doped into the network of a planar boron cluster and becomes an integral part of the molecular plane ($\text{Co} \in \text{B}_{18}^-$). Photoelectron spectroscopy reveals that CoB_{18}^- is an extremely stable electronic system with a very high electron binding energy. Global minimum searches coupled with high-level quantum chemical calculations have found that the most stable structure of CoB_{18}^- is planar and closed shell with C_{2v} (1A_1) symmetry, in which the monovalent Co atom is bonded with seven B atoms in its nearest neighbor and eleven additional B atoms in its second coordination shell. Chemical bonding analyses show that the planar CoB_{18}^- cluster has aromatic characters with ten delocalized π electrons. The Co atom is found to involve strong covalent interactions with the planar B_{18} host, as well as ionic bonding via metal to boron charge transfer. The planar CoB_{18}^- cluster represents a new class of metal-doped boron clusters, suggesting that metal atoms can be doped into the plane of monolayer borons to create metallo-borophenes with tunable magnetic, optical, and catalytic properties.

Acknowledgements

We thank Prof. A. I. Boldyrev and Prof. S. D. Li for invaluable discussions. The experimental work done at Brown University was supported by the National Science Foundation (CHE-1632813). The theoretical work done at Tsinghua University was supported by NKBRFSF (2013CB834603) and NSFC (21433005, 91426302, 21521091, and 21590792) of China. The calculations were performed using supercomputers at the Computer Network Information Center, Chinese Academy of Sciences, Tsinghua National Laboratory for Information Science and Technology, and Lüliang Tianhe-2 Supercomputing Center.

Keywords: ab initio calculation · boron clusters · chemical bonding · metallo-borophene · monovalent metal · photoelectron spectroscopy

How to cite: *Angew. Chem. Int. Ed.* **2016**, *55*, 7358–7363
Angew. Chem. **2016**, *128*, 7484–7489

- [1] B. Albert, H. Hillebrecht, *Angew. Chem. Int. Ed.* **2009**, *48*, 8640–8668; *Angew. Chem.* **2009**, *121*, 8794–8824.
- [2] W. N. Lipscomb, *Science* **1977**, *196*, 1047–1055.
- [3] A. N. Alexandrova, A. I. Boldyrev, H. J. Zhai, L. S. Wang, *Coord. Chem. Rev.* **2006**, *250*, 2811–2866.

- [4] E. Oger, N. R. M. Crawford, R. Kelting, P. Weis, M. M. Kappes, R. Ahlrichs, *Angew. Chem. Int. Ed.* **2007**, *46*, 8503–8506; *Angew. Chem.* **2007**, *119*, 8656–8659.
- [5] A. P. Sergeeva, I. A. Popov, Z. A. Piazza, W. L. Li, C. Romanescu, L. S. Wang, A. I. Boldyrev, *Acc. Chem. Res.* **2014**, *47*, 1349–1358.
- [6] H. J. Zhai, Y. F. Zhao, W. L. Li, Q. Chen, H. Bai, H. S. Hu, Z. A. Piazza, W. J. Tian, H. G. Lu, Y. B. Wu, Y. W. Mu, G. F. Wei, Z. P. Liu, J. Li, S. D. Li, L. S. Wang, *Nat. Chem.* **2014**, *6*, 727–731.
- [7] W. L. Li, R. Pal, Z. A. Piazza, X. C. Zeng, L. S. Wang, *J. Chem. Phys.* **2015**, *142*, 204305.
- [8] W. L. Li, Y. F. Zhao, H. S. Hu, J. Li, L. S. Wang, *Angew. Chem. Int. Ed.* **2014**, *53*, 5540–5545; *Angew. Chem.* **2014**, *126*, 5646–5651.
- [9] W. L. Li, Q. Chen, W. J. Tian, H. Bai, Y. F. Zhao, H. S. Hu, J. Li, H. J. Zhai, S. D. Li, L. S. Wang, *J. Am. Chem. Soc.* **2014**, *136*, 12257–12260.
- [10] Z. A. Piazza, H. S. Hu, W. L. Li, Y. F. Zhao, J. Li, L. S. Wang, *Nat. Commun.* **2014**, *5*, 3113.
- [11] I. Boustani, A. Quandt, E. Hernandez, A. Rubio, *J. Chem. Phys.* **1999**, *110*, 3176–3185.
- [12] M. H. Evans, J. D. Joannopoulos, S. T. Pantelides, *Phys. Rev. B* **2005**, *72*, 045434.
- [13] J. Kunstmass, A. Quandt, *Phys. Rev. B* **2006**, *74*, 035413.
- [14] K. C. Lau, R. Pandey, *J. Phys. Chem. C* **2007**, *111*, 2906–2912.
- [15] H. Tang, S. Ismail-Beigi, *Phys. Rev. Lett.* **2007**, *99*, 115501.
- [16] X. Yang, Y. Ding, J. Ni, *Phys. Rev. B* **2008**, *77*, 041402.
- [17] E. S. Penev, S. Bhowmick, A. Sadrzadeh, B. I. Yakobson, *Nano Lett.* **2012**, *12*, 2441–2445.
- [18] X. Wu, J. Dai, Y. Zhao, Z. Zhuo, J. Yang, X. C. Zeng, *ACS Nano* **2012**, *6*, 7443–7453.
- [19] Y. Liu, E. S. Penev, B. I. Yakobson, *Angew. Chem. Int. Ed.* **2013**, *52*, 3156–3159; *Angew. Chem.* **2013**, *125*, 3238–3241.
- [20] H. Liu, J. Gao, J. Zhao, *Sci. Rep.* **2013**, *3*, 3228.
- [21] Z. Zhang, Y. Yang, G. Gao, B. I. Yakobson, *Angew. Chem. Int. Ed.* **2015**, *54*, 13022–13026; *Angew. Chem.* **2015**, *127*, 13214–13218.
- [22] Different from the nomenclature of 2D elemental materials such as silicene, germanene, stanene, phosphorene, MXenes, and so on, borene has been used for organoboron compounds with B=B double bonds in chemistry and should not be confused with borophene for monolayer borons.
- [23] A. J. Mannix, X. F. Zhou, B. Kiraly, J. D. Wood, D. Alducin, B. D. Myers, X. Liu, B. L. Fisher, U. Santiago, J. R. Guest, M. J. Yacaman, A. Ponce, A. R. Oganov, M. C. Hersam, N. P. Guisinger, *Science* **2015**, *350*, 1513–1516.
- [24] a) B. J. Feng, J. Zhang, Q. Zhong, W. B. Li, S. Li, H. Li, P. Cheng, S. Meng, L. Chen, K. H. Wu, **2015**, arXiv:1512.05029; b) S. G. Xu, Y. J. Zhao, J. H. Liao, X. B. Yang, H. Xu, **2016**, arXiv:1601.01393.
- [25] G. A. Tai, T. Hu, Y. Zhou, X. Wang, J. Kong, T. Zeng, Y. You, Q. Wang, *Angew. Chem. Int. Ed.* **2015**, *54*, 15473–15477; *Angew. Chem.* **2015**, *127*, 15693–15697.
- [26] H. J. Zhai, A. N. Alexandrova, K. A. Birch, A. I. Boldyrev, L. S. Wang, *Angew. Chem. Int. Ed.* **2003**, *42*, 6004–6008; *Angew. Chem.* **2003**, *115*, 6186–6190.
- [27] R. Islas, T. Heine, K. Ito, P. v. R. Schleyer, G. Merino, *J. Am. Chem. Soc.* **2007**, *129*, 14767–14774.
- [28] B. B. Averkiev, A. I. Boldyrev, *Russ. J. Gen. Chem.* **2008**, *78*, 769–773.
- [29] J. C. Guo, W. Z. Yao, Z. Li, S. D. Li, *Sci. China Ser. B* **2009**, *52*, 566–570.
- [30] C. Romanescu, A. P. Sergeeva, W.-L. Li, A. I. Boldyrev, L. S. Wang, *J. Am. Chem. Soc.* **2011**, *133*, 8646–8653.
- [31] T. R. Galeev, C. Romanescu, W. L. Li, L. S. Wang, A. I. Boldyrev, *J. Chem. Phys.* **2011**, *135*, 104301.
- [32] W. L. Li, C. Romanescu, T. R. Galeev, L. S. Wang, A. I. Boldyrev, *J. Phys. Chem. A* **2011**, *115*, 10391–10397.
- [33] C. Romanescu, T. R. Galeev, W. L. Li, A. I. Boldyrev, L. S. Wang, *Acc. Chem. Res.* **2013**, *46*, 350–358.
- [34] T. R. Galeev, C. Romanescu, W. L. Li, L. S. Wang, A. I. Boldyrev, *Angew. Chem. Int. Ed.* **2012**, *51*, 2101–2105; *Angew. Chem.* **2012**, *124*, 2143–2147.
- [35] I. A. Popov, W. L. Li, Z. A. Piazza, A. I. Boldyrev, L. S. Wang, *J. Phys. Chem. A* **2014**, *118*, 8098–8105.
- [36] H. J. Zhai, B. Kiran, J. Li, L. S. Wang, *Nat. Mater.* **2003**, *2*, 827–833.
- [37] C. Xu, L. J. Cheng, J. L. Yang, *J. Chem. Phys.* **2014**, *141*, 124301.
- [38] N. Minh Tam, H. Tan Pham, L. Van Duong, P. H. M. Phuong, M. Tho Nguyen, *Phys. Chem. Chem. Phys.* **2015**, *17*, 3000–3003.
- [39] G. S. Nevill, S. Arta, B. I. Yakobson, *Phys. Rev. Lett.* **2007**, *98*, 166804.
- [40] a) Q. Chen, W. L. Li, Y. F. Zhao, S. Y. Zhang, H. S. Hu, H. Bai, H. R. Li, W. J. Tian, H. G. Lu, H. J. Zhai, S. D. Li, J. Li, L. S. Wang, *ACS Nano* **2015**, *9*, 754–760; b) Y. J. Wang, Y. F. Zhao, W.-L. Li, T. Jian, Q. Chen, X. R. You, T. Ou, X. Y. Zhao, H. J. Zhai, S. D. Li, J. Li, L. S. Wang, *J. Chem. Phys.* **2016**, *144*, 064307.
- [41] H. Bai, Q. Chen, H. J. Zhai, S. D. Li, *Angew. Chem. Int. Ed.* **2015**, *54*, 941–945; *Angew. Chem.* **2015**, *127*, 955–959.
- [42] P. Jin, Q. Hou, C. Tang, Z. Chen, *Theor. Chem. Acc.* **2015**, *134*, 13.
- [43] W. Fa, S. Chen, S. Pande, X. C. Zeng, *J. Phys. Chem. A* **2015**, *119*, 11208–11214.
- [44] A. A. Popov, S. Yang, L. Dunsch, *Chem. Rev.* **2013**, *113*, 5989–6113.
- [45] I. A. Popov, T. Jian, G. V. Lopez, A. I. Boldyrev, L. S. Wang, *Nat. Commun.* **2015**, *6*, 8654.
- [46] J. Li, X. Li, H. J. Zhai, L. S. Wang, *Science* **2003**, *299*, 864–867.
- [47] H. J. Zhai, B. Kiran, B. Dai, J. Li, L. S. Wang, *J. Am. Chem. Soc.* **2005**, *127*, 12098–12106.
- [48] P. Schipper, O. Gritsenko, S. van Gisbergen, E. Baerends, *J. Chem. Phys.* **2000**, *112*, 1344.
- [49] P. Pyykkö, *J. Phys. Chem. A* **2015**, *119*, 2326–2337.
- [50] C. Romanescu, T. R. Galeev, W. L. Li, A. I. Boldyrev, L. S. Wang, *Angew. Chem. Int. Ed.* **2011**, *50*, 9334–9337; *Angew. Chem.* **2011**, *123*, 9506–9509.
- [51] W. L. Li, C. Romanescu, Z. A. Piazza, L. S. Wang, *Phys. Chem. Chem. Phys.* **2012**, *14*, 13663–13669.
- [52] A. P. Sergeeva, B. B. Averkiev, H. J. Zhai, A. I. Boldyrev, L. S. Wang, *J. Chem. Phys.* **2011**, *134*, 224304.
- [53] D. Y. Zubarev, A. I. Boldyrev, *Phys. Chem. Chem. Phys.* **2008**, *10*, 5207–5217.
- [54] P. Cui, H. S. Hu, B. Zhao, J. T. Miller, P. Cheng, J. Li, *Nat. Commun.* **2015**, *6*, 6331.
- [55] H. C. Hu, H. S. Hu, B. Zhao, P. Cui, P. Cheng, J. Li, *Angew. Chem. Int. Ed.* **2015**, *54*, 11681–11685; *Angew. Chem.* **2015**, *127*, 11847–11851.

Received: February 12, 2016

Revised: March 16, 2016

Published online: April 20, 2016